

# Differential Binding of RhoA, RhoB, and RhoC to Protein Kinase C-Related Kinase (PRK) Isoforms PRK1, PRK2, and PRK3: PRKs Have the Highest Affinity for RhoB

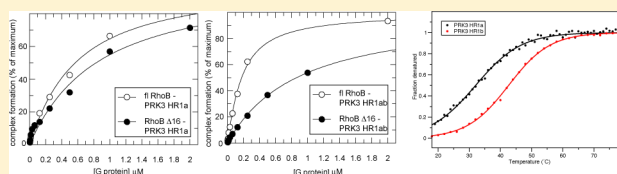
Catherine L. Hutchinson,<sup>†,||</sup> Peter N. Lowe,<sup>‡</sup> Stephen H. McLaughlin,<sup>†,§</sup> Helen R. Mott,<sup>†</sup> and Darerca Owen<sup>\*,†</sup>

<sup>†</sup>Department of Biochemistry, University of Cambridge, 80 Tennis Court Road, Cambridge CB2 1GA, U.K.

<sup>‡</sup>Biomolecular Interactions Consultancy, 3 Danesbury Park, Hertford SG14 3HX, U.K.

<sup>§</sup>MRC Laboratory of Molecular Biology, Francis Crick Avenue, Cambridge Biomedical Campus, Cambridge CB2 0QH, U.K.

**ABSTRACT:** Protein kinase C-related kinases (PRKs) are members of the protein kinase C superfamily of serine-threonine kinases and can be activated by binding to members of the Rho family of GTPases via a Rho-binding motif known as an HR1 domain. Three tandem HR1 domains reside at the N-terminus of the PRKs. We have assessed the ability of the HR1a and HR1b domains from the three PRK isoforms (PRK1, PRK2, and PRK3) to interact with the three Rho isoforms (RhoA, RhoB, and RhoC). The affinities of RhoA and RhoC for a construct encompassing both PRK1 HR1 domains were similar to those for the HR1a domain alone, suggesting that these interactions are mediated solely by the HR1a domain. The affinities of RhoB for both the PRK1 HR1a domain and the HR1ab didomain were higher than those of RhoA or RhoC. RhoB also bound more tightly to the didomain than to the HR1a domain alone, implicating the HR1b domain in the interaction. As compared with PRK1 HR1 domains, PRK2 and PRK3 domains bind less well to all Rho isoforms. Uniquely, however, the PRK3 domains display a specificity for RhoB that requires both the C-terminus of RhoB and the PRK3 HR1b domain. The thermal stability of the HR1a and HR1b domains was also investigated. The PRK2 HR1a domain was found to be the most thermally stable, while PRK2 HR1b, PRK3 HR1a, and PRK3 HR1b domains all exhibited lower melting temperatures, similar to that of the PRK1 HR1a domain. The lower thermal stability of the PRK2 and PRK3 HR1b domains may impart greater flexibility, driving their ability to interact with Rho isoforms.



The Ras superfamily small G proteins are molecular switches that utilize the binding and hydrolysis of GTP to control signal transduction pathways. GTP binding drives a conformational change that permits the G protein to interact with downstream effector proteins, mediating a range of cellular responses. The Rho family small G proteins control a wide range of signaling pathways and are best known for their involvement in cell adhesion, growth, and motility through their control of the actin cytoskeleton.<sup>1</sup> Due to their integral role in the regulation of the actin cytoskeleton, Rho family proteins also contribute to pathological processes, including various neuro-developmental disorders such as Fragile X syndrome and Williams syndrome,<sup>2</sup> Alzheimer's disease,<sup>3</sup> and multiple sclerosis;<sup>4</sup> cardiovascular diseases such as hypertension, atherosclerosis, and heart failure;<sup>5</sup> and cell invasion and metastasis in cancer.<sup>6</sup> Rho family proteins are in fact upregulated in many types of human tumors.<sup>6</sup> Understanding how Rho family members contribute to the transforming potential of cells, through deregulation of their signaling pathways at a molecular level, could potentially lead to the development of therapeutics for tackling a wide range of human diseases.

The cellular functions of the Rho proteins are initiated by their interaction with their immediate downstream effector

proteins. The PRK family of serine-threonine kinases is one such effector group. PRKs have been implicated in the control of a number of important cellular pathways.

PRK1 mediates control of the cytoskeletal network through phosphorylation of the intermediate filament proteins, neurofilament (subunits L, M, and H), and vimentin.<sup>7,8</sup> The microfilament protein,  $\alpha$ -actinin, is also a substrate for PRK1.<sup>9</sup> PRK1 has been observed to accumulate in neurofibrillary tangles associated with Alzheimer's disease.<sup>10</sup> Moreover, PRK1 plays a role in cancer progression: it is overexpressed in prostate cancer and has been shown to enhance the transcriptional activity of the androgen receptor by phosphorylating histone H3.<sup>11,12</sup> Additionally, PRK1 has been shown to phosphorylate the human papilloma virus E6 oncoprotein, incriminating it in virally induced cancers.<sup>13</sup>

PRK2 has also been shown to regulate cytoskeletal substrates; it can phosphorylate cortactin, weakening its ability to cross-link F-actin.<sup>14</sup> This isoform has also been shown to be involved in cell migration and invasion in bladder cancer cell lines.<sup>15</sup> Interestingly, PRK2 has recently been shown to play a

**Received:** September 3, 2013

**Revised:** October 2, 2013

**Published:** October 15, 2013

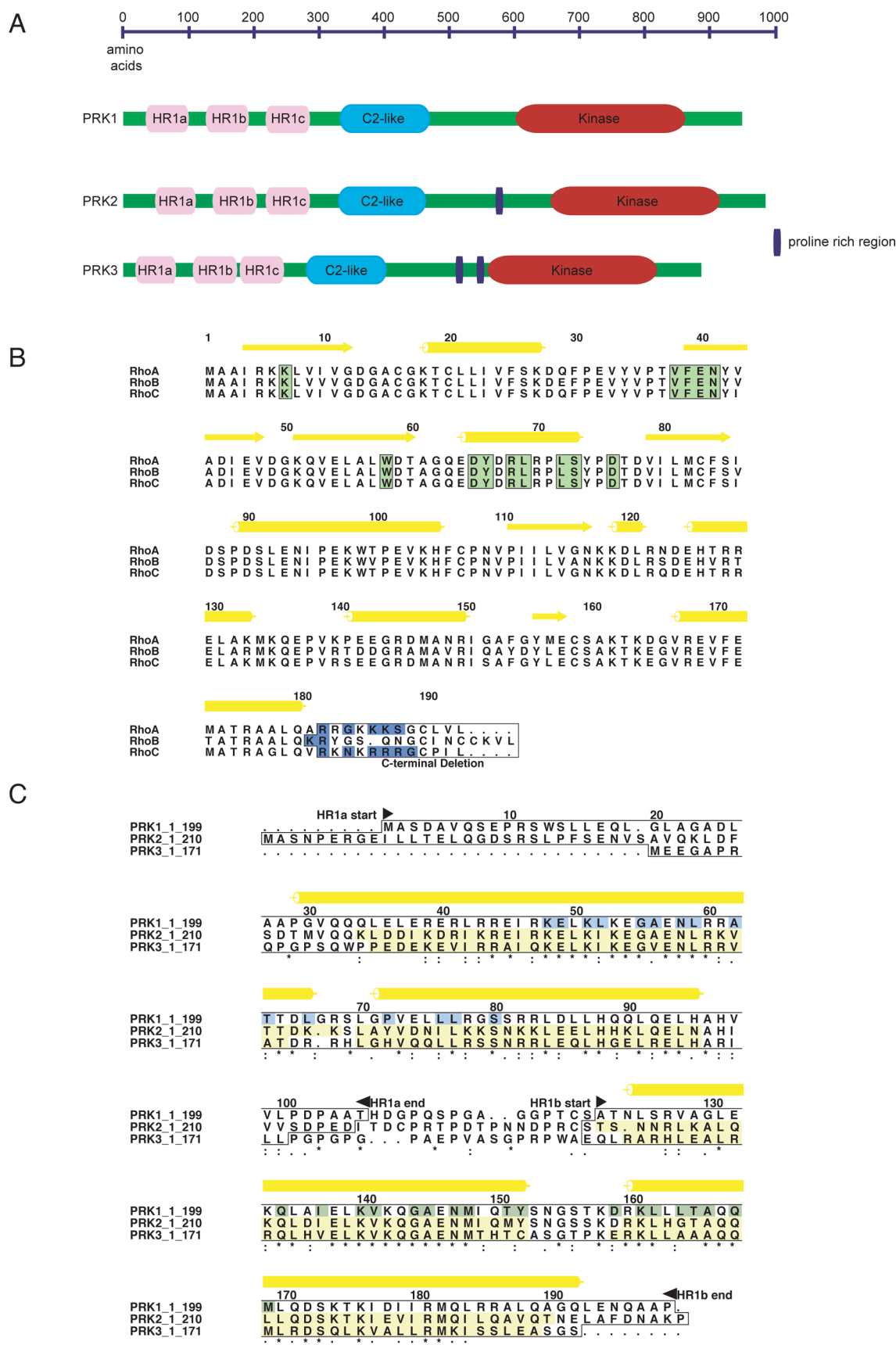


**Figure 1.** Domain structure of PRKs and sequence alignments of the three isoforms of PRK and Rho. (A) Domain structure of PRK1, PRK2, and PRK3. PRK isoforms contain three tandem HR1 domains at their N-termini, a calcium binding C2-like domain and a C-terminal PKC-like serine/threonine kinase domain. The limits of all domains are taken from the SMART database, except for the HR1a and HR1b domains of PRK1 where the limits are taken from the structures (PDB entries 1CXZ and 1URF, respectively). PRK2 and PRK3 also contain one and two proline-rich regions,

Figure 1. continued

respectively, which contain minimal SH3 domain recognition consensus sequences. (B) Sequence alignment of human RhoA, RhoB, and RhoC. The conserved secondary structure of the proteins is indicated by yellow cylinders ( $\alpha$ -helices) and arrows ( $\beta$ -strands) above the alignment. The residues in RhoA that are known to interact with PRK1 (contact II site) are highlighted in green. The residues at the C-terminus that were removed to form the truncated versions of the proteins are boxed. The basic residues in the C-terminal hypervariable region are colored blue. Panels B and C were produced with Alscript.<sup>54</sup> (C) Sequence alignment of human PRK1, PRK2, and PRK3. The sequences of the HR1ab constructs used are shown, aligned using ClustalX. The limits of the HR1a and HR1b domain constructs are indicated by boxes and black arrows above the sequences. The experimentally determined helices in PRK1 are represented as yellow cylinders above the alignment. The PRK1 residues are numbered above the alignment. The positions of helices predicted by JPred in PRK2 and PRK3 are highlighted in pale yellow. HR1a residues involved in contacts with RhoA are highlighted in blue. HR1b residues involved in contacts with Rac1 are highlighted in green. The conservation is indicated below the alignment according to ClustalX as follows: asterisks for identical residues at all positions, colons for full conservation of a strong group, and periods for full conservation of a weak group.

role in cell cycle progression. It is required for activation of Cdc25B, which allows the G2 to M transition and is also required for abscission to occur allowing exit from cytokinesis into G1.<sup>16</sup> PRK2 has also been implicated in the regulation of E-cadherin-dependent cell–cell adhesion in keratinocytes<sup>17</sup> and has, more specifically, been shown to be required for maturation of apical junctions in epithelial cells.<sup>18</sup>

PRK3 is the least well studied of the three PRK isoforms. Although reports vary, ubiquitous expression of PRK1 and PRK2 in adult mammalian tissues has been shown;<sup>19,20</sup> however, PRK3 expression appears to be more restricted in normal tissue<sup>21</sup> but easily detectable in multiple cancer cell lines.<sup>22</sup> PRK3 has been shown to be activated downstream of PI3 kinase, in which context it contributes to the invasive properties of prostate cancer cell lines.<sup>23</sup> Furthermore, it has also been shown to regulate actin dynamics, controlling migration and adhesion in endothelial cells,<sup>24,25</sup> and in conjunction with RhoC, PRK3 has been demonstrated to sustain an advanced malignant phenotype in breast cancer cells.<sup>26</sup> The only substrates identified for PRK3 to date are the microtubule regulator protein CLIP-170 and the EGF receptor.<sup>27</sup>

A growing body of evidence, described above, suggests that all three PRK isoforms have similar functional roles, ultimately underpinned by control of the actin cytoskeleton, leading to their control of cell morphology, cell motility, and cell–cell junction regulation. Although exhaustive studies looking for pathways controlling PRK activation are yet to be undertaken, each isoform appears to respond to different stimuli, and they do not appear to have redundant roles in the cell. PRK1 is involved in androgen receptor signaling (along with signaling from other nuclear receptor pathways)<sup>11</sup> and is activated downstream of PAR-1.<sup>28</sup> PRK2 is activated in response to CD44 stimulation,<sup>14</sup> while PRK3 responds to insulin.<sup>23</sup>

The interaction of Rho proteins with their downstream effectors is mediated by recognition motifs known as Rho-binding domains (RBDs). There are at least three classes of RBD. Class I motifs are found in the protein kinase C-related kinases (PRKs), along with the Rhotekins and the Rhoophilins. Class II includes the RBDs in the Rho-associated kinases (ROCKs/ROKs), and class III includes that in Citron.<sup>29</sup> The class I RBDs, also known as HR1 or REM domains, were first identified in serine-threonine kinase PRK1.<sup>21,30</sup> The PRK proteins, PRK1 (PKN or PKN $\alpha$ ), PRK2 (PKN $\gamma$ ), and PRK3 (PKN $\beta$ ), have the same overall domain architecture (Figure 1A). Their N-terminal regions contain three tandem HR1 domains, HR1a, HR1b, and HR1c. These are followed by a C2-like domain that is related to the calcium-dependent membrane targeting domain in protein kinase C and a C-terminal kinase

domain that is a member of the protein kinase C superfamily.<sup>31</sup> The main difference between PRK1 and the two other family members is that both PRK2 and PRK3 contain proline-rich regions in the linker between the C2-like domain and the catalytic domain, and these regions contain the minimal consensus sequence for SH3 domain recognition (Figure 1A).

Structural studies have shown that both the HR1a and HR1b domains from PRK1 form antiparallel coiled coils.<sup>32,33</sup> The HR1a domain has been shown to bind to both RhoA and Rac1 with high affinity.<sup>33–35</sup> The X-ray structure of RhoA in complex with HR1a identified two potential contact interfaces between the RBD and the small G protein, termed contact I and contact II. Mutagenesis work conducted to determine whether both of the identified contact interfaces could be occupied in solution demonstrated that contact II, encompassing the switch regions, was the relevant binding interface for RhoA.<sup>36</sup>

The HR1b domain of PRK1 can bind tightly to only Rac1,<sup>33</sup> and the solution structure of Rac1 in complex with the PRK1 HR1b domain revealed a single interaction interface, similar to the nucleotide-dependent contact II observed in the RhoA–HR1a structure.<sup>37</sup>

The sequence of the HR1c domain of PRK1 is less similar to that of HR1a or HR1b than the sequences of HR1a and HR1b are to each other. Consistent with this divergence, HR1c is unable to bind RhoA.<sup>34</sup> The functional role of the HR1c domains in the PRKs is currently unknown.

The work presented here extends our previous dissection of the PRK1–RhoA interaction<sup>36</sup> to include the interactions of the HR1a and HR1b domains from PRK1 with RhoB and RhoC, along with the interactions of the HR1a and HR1b domains of the two other members of the PRK family, PRK2 and PRK3, with all three Rho isoforms. The minimal interaction region in PRK2 and PRK3 responsible for binding to Rho family proteins has never been formally delineated, but it is likely that PRK2 and PRK3 interact with Rho family G proteins through their HR1 domains. PRK2 has been shown to bind to RhoA, Rac1, and Rac2 in a GTP-dependent manner.<sup>20,38,39</sup> Mutations in the HR1a and HR1b domains of PRK2 have also been shown to abrogate binding to RhoA.<sup>18</sup> A direct interaction has been reported between *in vitro*-translated PRK3 and RhoA,<sup>22</sup> while PRK3 has also been shown to bind to RhoA, RhoB, and RhoC by co-immunoprecipitation.<sup>26</sup>

It seems likely that a range of cellular responses to extracellular signals is controlled through the Rho family proteins activating distinct PRK isoforms, which then signal to different downstream targets.<sup>7,10,13,17,40</sup> To try to elucidate which Rho small G proteins may activate distinct PRKs, we have investigated the interaction of the HR1 domains of all three PRK isoforms with all three Rho GTPases using direct

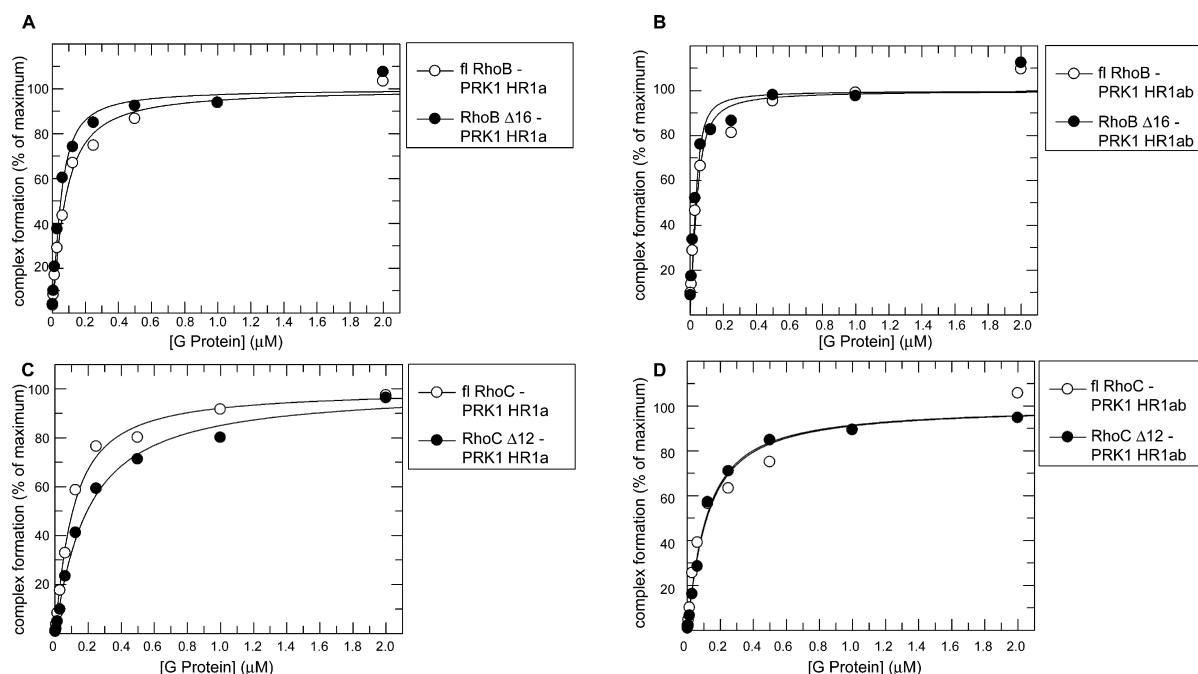


**Figure 2.** SPA binding data for full-length and truncated RhoB and RhoC with PRK1 HR1a and HR1ab. The indicated concentration of [ $^3$ H]GTP-labeled G protein was incubated with the His-tagged effector protein in each SPA. The SPA signal was corrected by subtraction of the background signal from parallel measurements in which the effector protein was omitted. The effect of the concentration of G protein on this corrected SPA signal was fit to a binding isotherm to give an apparent  $K_d$  value and the signal at saturating G protein concentrations. The data and curve fits are displayed as a percentage of this maximal signal: (A) binding isotherms of full-length and truncated RhoB with PRK1 HR1a, (B) binding isotherms of full-length and truncated RhoB with PRK1 HR1ab, (C) binding isotherms of full-length and truncated RhoC with PRK1 HR1a, and (D) binding isotherms of full-length and truncated RhoC with PRK1 HR1ab.

binding experiments. We also present data describing the biophysical properties of the HR1 domains and relate them to their ability to bind to Rho family small G proteins.

## MATERIALS AND METHODS

**Expression Constructs.** *Homo sapiens* full-length RhoA (residues 1–193), truncated RhoA (residues 1–181), full-length RhoB (residues 1–196), truncated RhoB (residues 1–180), full-length RhoC (residues 1–193), and truncated RhoC (residues 1–181), all with F25N and Q63L mutations, were expressed as glutathione S-transferase (GST) fusion proteins in the pGEX-2T expression vector (GE Healthcare) by cloning the coding regions into the *Bam*HI and *Eco*RI sites of the vector.

Constructs expressing *H. sapiens* PRK1 HR1a (residues 1–106), PRK1 HR1b (residues 122–199), and PRK1 HR1ab (residues 1–199) have been described previously.<sup>36</sup> *H. sapiens* PRK2 HR1a (residues 1–114), PRK2 HR1b (residues 132–210), PRK2 HR1ab (residues 1–210), PRK3 HR1a (residues 1–80), PRK3 HR1b (residues 100–171), and PRK3 HR1ab (residues 1–171) were amplified by polymerase chain reaction (introducing the relevant restriction sites into the primers) and cloned into the *Bam*HI and *Eco*RI sites of a modified pGEX-4T3 vector.<sup>36</sup> This vector produces proteins with a cleavable N-terminal GST tag and a permanent C-terminal His tag. The *H. sapiens* PRK2 template was a kind gift from P. Parker (LRI, London, U.K.). The *H. sapiens* PRK3 template was IMAGE clone 6649806, purchased from Geneservice Ltd.

**Recombinant Protein Production.** GST fusion proteins were expressed in *Escherichia coli* BL21 (Novagen Inc.). Stationary cultures were diluted 1:10 and grown at 37 °C to an  $A_{600}$  of 0.8, and protein expression was induced by the

addition of 0.1 mM IPTG for 16 h at 20 °C. Proteins were then purified using glutathione agarose beads (Sigma-Aldrich) following the manufacturer's instructions. Rho isoforms were cleaved from their GST tag while attached to the beads using thrombin (Merck). GST-HR1-His domains were eluted from the glutathione beads and cleaved from the GST tag using PreScission protease (GE Healthcare), and the His-tagged HR1 domains were purified using Ni-IDA resin (Novagen). All proteins were further purified by gel filtration on a Superdex 75 16/60 HiLoad gel filtration column (GE Healthcare), prior to use in assays. Protein concentrations for the Rho proteins were evaluated from measurement of their  $A_{280}$  using their amino acid composition and the extinction coefficients of tyrosine, tryptophan, and the guanine nucleotide.<sup>41</sup> The concentrations for the HR1 domains were determined using amino acid analysis in the Protein and Nucleic Acid Chemistry facility at the Department of Biochemistry, University of Cambridge.

**Nucleotide Exchange.** Rho proteins were labeled with [ $^3$ H]GTP for use in binding assays as described previously.<sup>42</sup>

**Scintillation Proximity Assays (SPAs).** Affinities of Rho proteins for the HR1-His domains were measured using SPA. The His-tagged effector proteins, at constant concentrations (60 nM PRK1 HR1a, 100 nM PRK1 HR1ab, 150 nM PRK2 HR1a/ab, and 150 nM PRK3 HR1a/ab), were immobilized on Protein A SPA fluoromicrospheres via an anti-His antibody (Sigma-Aldrich). The equilibrium binding constants ( $K_d$ ) of the effector–G protein interaction were determined by monitoring the SPA signal in the presence of varying concentrations of [ $^3$ H]GTP-Rho, as described previously.<sup>43</sup> Binding of Rho to the effector protein brings the radiolabeled nucleotide close enough to the scintillant to obtain a signal. For each Rho variant, an experiment was performed in the absence of effector, which



**Table 1. Affinities of the Rho Isoforms for the PRK HR1 Domains<sup>a</sup>**

	apparent $K_d$ (nM)					
	PRK1		PRK2		PRK3	
	HR1a	HR1ab	HR1a	HR1ab	HR1a	HR1ab
RhoA fl	150 ± 20	140 ± 15	493 ± 75	~1390 ± 51 <sup>b</sup>	424 ± 72	704 ± 110
RhoA Δ12	60 ± 8	50 ± 6	532 ± 55	807 ± 77	400 ± 77	235.8 ± 58
RhoB fl	52 ± 7	15 ± 5	450 ± 53	434 ± 42	496 ± 128	127 ± 9
RhoB Δ16	26 ± 5	8 ± 4	686 ± 89	211 ± 38	757 ± 205	812 ± 70
RhoC fl	82 ± 10	90 ± 22	~1511 ± 147	~14200 ± 2150	~3060 ± 527	716 ± 64
RhoC Δ12	169 ± 21	93 ± 12	~1291 ± 108	~1634.2 ± 151	~1150 ± 282	550 ± 105

<sup>a</sup>Equilibrium binding constants were determined in SPAs as described in Materials and Methods.  $K_d$  values are quoted with the standard errors from curve fitting. <sup>b</sup> $K_d$  values of >1000 nM (1 μM) are based on data from which it was not possible to achieve sufficiently high concentrations to obtain a full binding curve. As such,  $K_d$  values are subject to errors.

resulted in a linear increase in background SPA counts. This data set was then subtracted from the data points obtained in the presence of effector and plotted as a function of increasing concentration of Rho protein. For each affinity determination, data points were obtained for at least 10 different G protein concentrations. Binding curves were fit using a direct binding isotherm<sup>43</sup> to obtain  $K_d$  values and their standard errors for the G protein–effector interactions.

**Circular Dichroism (CD).** The secondary structure and thermal stability were assessed by CD. Free HR1 domains were buffer exchanged into 10 mM potassium phosphate (pH 7.5) and 100 mM sodium fluoride. Spectra were recorded on an AVIV 410 instrument at a protein concentration of 0.1 mg/mL in a 0.1 cm path-length quartz cuvette at 18 °C. Three wavelength scans were recorded for each protein between 250 and 180 nm. Secondary structure prediction was performed on DICHROWEB<sup>44,45</sup> using CDSSTR<sup>46,47</sup> and reference set 3. The thermal stability was determined by following the temperature dependence of the absorbance signal of the HR1 domains at 222 nm between 18 and 80 °C in 2 °C increments with a 30 s equilibration time. The fraction of denatured protein was calculated as described previously.<sup>36</sup>

## RESULTS

**RhoA, RhoB, and RhoC Constructs.** Our previous work investigating the interaction between RhoA and the HR1a, HR1b, and HR1ab domains of PRK1 utilized a C-terminal truncation of RhoA (residues 1–186); this truncation removes the lipid modification signal from the G protein, together with part of the polybasic sequence.<sup>36</sup> We also utilized the F25N mutation that aids the solubility of the protein and the Q63L mutation that maintains the small G protein in the active, GTP-bound conformation, required for the interaction with effector proteins. A careful assessment of the RhoA sequence led us to believe that a further truncation, removing the complete polybasic sequence, would be valuable; thus, we produced RhoA 1–181 (F25N/Q63L), hereafter RhoA Δ12. To allow a fair comparison of the Rho family proteins, we produced similar truncations in RhoB (residues 1–180, RhoB Δ16) and RhoC (residues 1–181, RhoC Δ12) and also introduced the F25N and Q63L mutations into these proteins (Figure 1B).

**The Rho Isoforms Have Different Affinities for the PRK1 HR1 Domains.** The apparent  $K_d$  values for the interaction between the PRK1 HR1a and PRK1 HR1ab domains and Rho isoforms RhoA, RhoB, and RhoC were determined by SPA. The binding isotherms are shown in Figure 2, and the affinities are summarized in Table 1. The affinity of

RhoA Δ12 for PRK1 HR1a was 60 nM and for HR1ab was 50 nM. These are comparable with our previous estimations using the shorter truncation, RhoA Δ7.<sup>36</sup> RhoB Δ16 binds PRK1 HR1a with an affinity of 26 nM and PRK1 HR1ab with an affinity of 8 nM, while RhoC Δ12 binds PRK1 HR1a with an affinity of 169 nM and PRK1 HR1ab with an affinity of 93 nM. Thus, truncated RhoB appears to bind more tightly to PRK1 than truncated RhoA, while truncated RhoC binds slightly more weakly. It was also notable that RhoB Δ16 and, to a lesser extent, RhoC Δ12 bind more tightly to PRK1 HR1ab, implying that the HR1b domain is contributing to the affinity of the interaction with RhoB (and maybe RhoC) but not to RhoA.

**C-Terminal Truncation of the Rho Isoforms Does Not Affect the Binding of PRK1 HR1 Domains.** The majority of the amino acid sequence variation between the Rho isoforms occurs near the C-terminus,<sup>48</sup> more specifically within the C-terminal polybasic region (Figure 1B). We have reported previously that the interaction between Rac1 and PRK1 HR1b requires the C-terminal polybasic region of Rac1 but that the interaction between RhoA and PRK1 HR1a or PRK1 HR1ab does not require the equivalent region.<sup>33</sup> To determine whether the C-terminal polybasic regions of RhoB and/or RhoC were involved in the interaction with the PRK1 HR1 domains, we determined the affinities of full-length RhoA, RhoB, and RhoC for PRK1 HR1a and HR1ab. The results are summarized in Table 1, and the binding isotherms are shown in Figure 2.

By comparing the apparent  $K_d$  values for binding to full-length and truncated Rho proteins, it is clear that the inclusion of the C-terminal polybasic region has little effect on the binding of the Rho isoforms to PRK1 HR1 domains. Hence, it is not the sequence variation or the alteration of the charge state in this region that drives the tighter interaction between RhoB and PRK1. For RhoA and RhoB, in these data and in previous studies, we observe slightly lower apparent  $K_d$  values for the truncated G proteins binding to HR1 domains, which we interpret to be due to the increased stability of the truncated proteins. While full-length RhoC does appear to bind more tightly than RhoC Δ12 to PRK1 HR1a, no differences are seen with the PRK1 HR1ab didomain. Thus, the C-terminal regions of RhoA, RhoB, and RhoC do not appear to be involved in binding to PRK1, and full-length RhoB displays the highest binding affinity of all Rho isoforms, just as we observe for the truncated isoforms.

**HR1 Domains of PRK2 and PRK3.** Most of the published work on the interaction of PRK2 and PRK3 with Rho family small G proteins has used mammalian cell lysates to perform pull-down experiments with full-length PRK isoforms. To date, there has been no work on the isolated HR1 domains. The

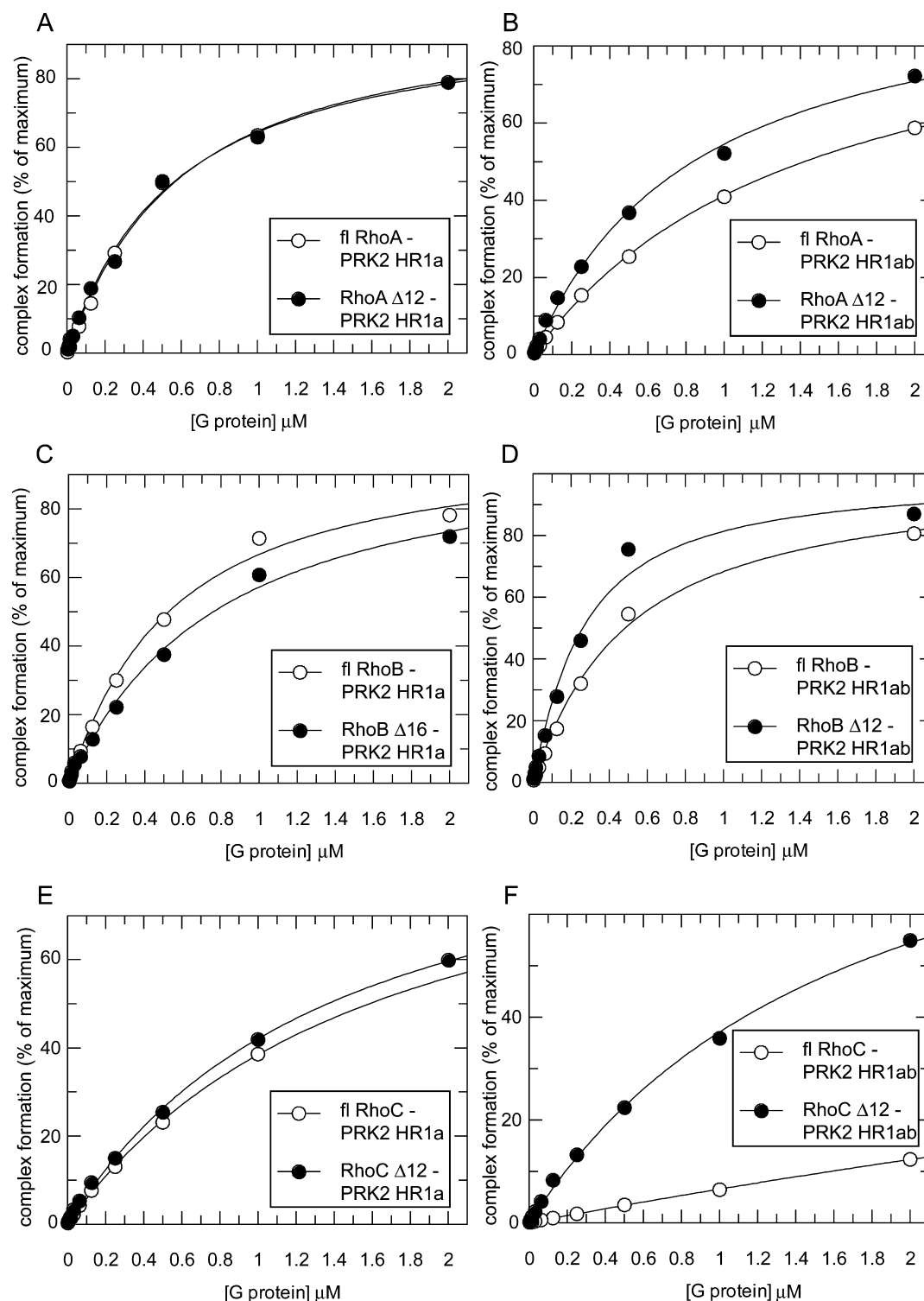


**Figure 3.** SPA binding data for full-length and truncated RhoA, RhoB, and RhoC with PRK2 HR1a and HR1ab. The indicated concentration of the [ $^3\text{H}$ ]GTP-labeled G protein was incubated with the His-tagged effector protein in each SPA. The SPA signal was corrected by subtraction of the background signal from parallel measurements in which the effector protein was omitted. The effect of the concentration of G protein on this corrected SPA signal was fit to a binding isotherm to give an apparent  $K_d$  value and the signal at saturating G protein concentrations. The data and curve fits are displayed as a percentage of this maximal signal: (A) binding isotherms of full-length and truncated RhoA with PRK2 HR1a, (B) binding isotherms of full-length and truncated RhoA with PRK2 HR1ab, (C) binding isotherms of full-length and truncated RhoB with PRK2 HR1a, (D) binding isotherms of full-length and truncated RhoB with PRK2 HR1ab, (E) binding isotherms of full-length and truncated RhoC with PRK2 HR1a, and (F) binding isotherms of full-length and truncated RhoC with PRK2 HR1ab.

HR1 domains of the three PRK isoforms share 43–68% identical sequences with one another.<sup>21,22</sup> The amino acid sequences of PRK2 and PRK3 were analyzed by FUGUE<sup>49</sup> to

identify homology to PRK1 based on the published structures of the HR1a and HR1b domains.<sup>32,33</sup> These data were used to generate a secondary structure mask, which was then applied to

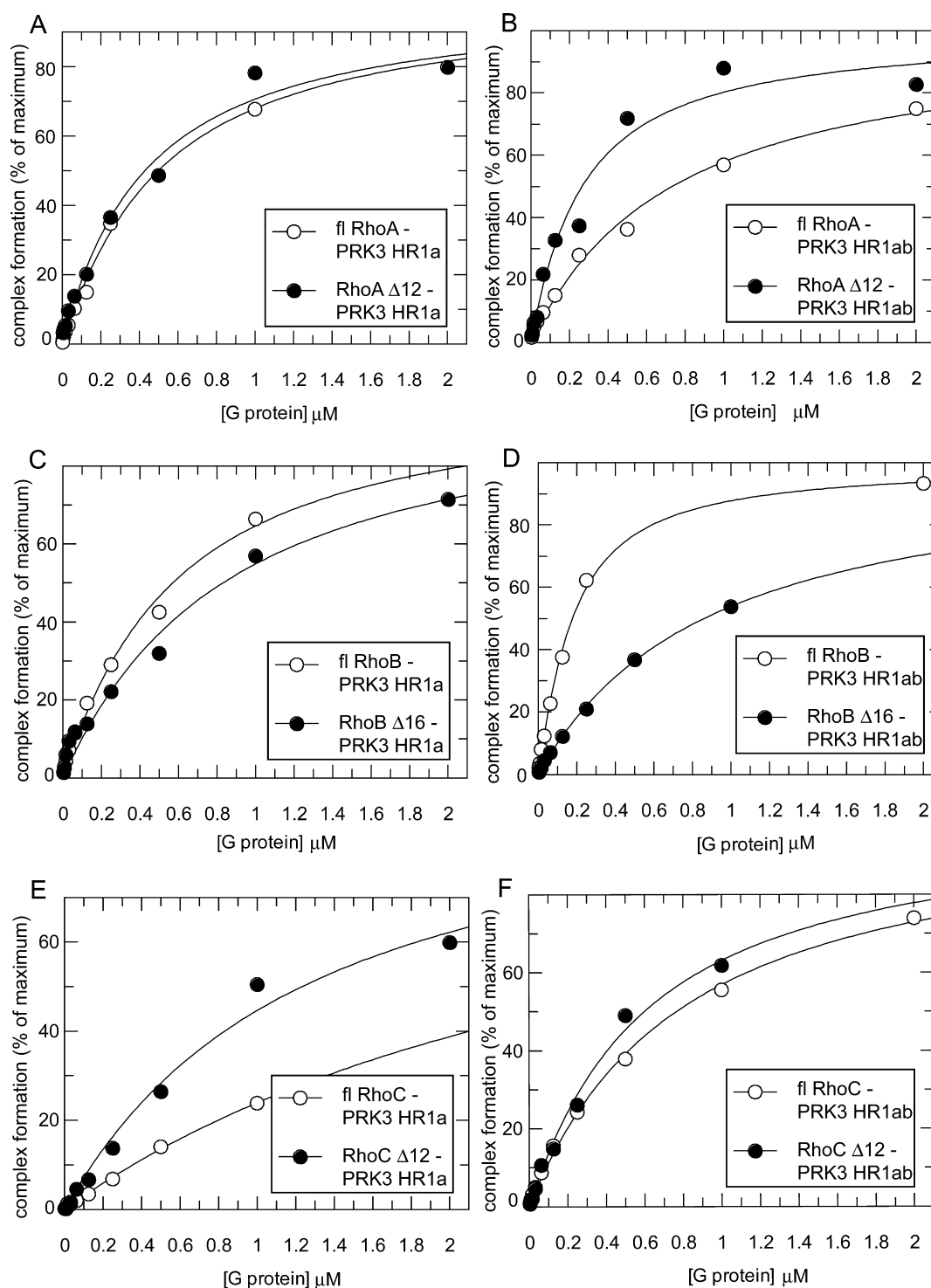


**Figure 4.** SPA binding data for full-length and truncated RhoA, RhoB, and RhoC with PRK2 HR1a and HR1ab. The experimental details are the same as for Figure 3. The data and curve fits are displayed as a percentage of this maximal signal: (A) binding isotherms of full-length and truncated RhoA with PRK3 HR1a, (B) binding isotherms of full-length and truncated RhoA with PRK3 HR1ab, (C) binding isotherms of full-length and truncated RhoB with PRK3 HR1a, (D) binding isotherms of full-length and truncated RhoB with PRK3 HR1ab, (E) binding isotherms of full-length and truncated RhoC with PRK3 HR1a, and (F) binding isotherms of full-length and truncated RhoC with PRK3 HR1ab.

the PRK1 amino acid sequence before a pairwise alignment was performed using ClustalX.<sup>50,51</sup> These alignments were used to identify the limits of the HR1 domain constructs that were cloned from PRK2 and PRK3 (Figure 1C).

**Interaction between PRK2 and the Rho Isoforms.** The affinities of the PRK2 HR1a domain and HR1ab didomain were determined for the three Rho isoforms (RhoA, RhoB, and

RhoC) by SPA. The affinities of the PRK2 domains for both the full-length and C-terminal truncation mutants of the Rho isoforms were determined in the same manner as for the PRK1 HR1 domains. The affinities are summarized in Table 1, and the binding isotherms for the interactions are shown in Figure 3.

The HR1 domains from PRK2 bind to all three Rho isoforms with 5–10-fold lower affinities than the HR1 domains from PRK1. With PRK2, RhoA and RhoB bind with similar affinities to the HR1a domain, while the interaction with RhoC is weaker. This contrasts with the selectivity for PRK1, where RhoA and RhoC had similar affinity but RhoB displayed tighter binding.

The affinities of the full-length and truncated RhoA and RhoC isoforms for the PRK2 HR1ab didomain were comparable to the affinities for the HR1a domains alone. This was also the case for the interaction of full-length RhoB with the PRK2 HR1ab didomain. Interestingly, however, RhoB  $\Delta$ 16 binds to the PRK2 HR1ab didomain with a 3.3-fold increase in affinity compared to that with the HR1a domain alone.

There is no evidence to suggest that the C-termini of any of the three Rho isoforms are involved in the interactions with PRK2 as in all cases the binding affinities for the full-length and truncated Rho proteins are similar or weaker.

### Interaction between PRK3 and the Rho Isoforms.

Finally, the affinities of the PRK3 HR1a and HR1ab domains were determined for the three Rho isoforms, in both the full-length and truncated forms. The affinities are summarized in Table 1, and the binding isotherms for the interactions are shown in Figure 4.

As for PRK2, the affinities of the Rho isoforms for PRK3 were generally weaker than those determined for PRK1. Again RhoA and RhoB bound with measurable and similar affinities for PRK3 HR1a, similar to those for PRK2. RhoC displayed very weak binding for PRK3 HR1a, just as for PRK2, but stronger binding was observed for PRK3 HR1ab. The data for binding of RhoB to PRK3 demonstrate some very interesting features. Comparison of the affinities of the full-length and C-terminally truncated RhoB proteins showed that full-length RhoB bound to both the PRK3 HR1a and HR1ab didomain with increased affinity; in particular, the affinity for the HR1ab domain is 6-fold higher for full-length RhoB than for truncated RhoB. This suggests that there may be a role for the C-terminus of RhoB in binding to PRK3. Equally interestingly, we observed a 4-fold increase in the affinity of full-length RhoB for HR1ab versus that for HR1a, suggesting a role for the HR1b domain in the RhoB interaction.

**Analysis of the Biophysical Properties of the PRK2 and PRK3 HR1 Domains.** Our previous work investigating the biophysical properties of the PRK1 HR1 domains provided some insight into why HR1a and HR1b bind differently to small G proteins.<sup>36</sup> The HR1 domains from PRK2 and PRK3 do not have the same affinity for Rho proteins as the PRK1 HR1 domains, and therefore, the percentage of secondary structure and thermal stabilities of the PRK2 and PRK3 HR1 domains were determined by CD to confirm that the domains were folded and to start to investigate why the PRK2 and PRK3 HR1 domains bind to the Rho isoforms with a lower affinity than the PRK1 HR1 domains.

Since no structural data are available for the PRK2 or PRK3 HR1 domains, data from JPred secondary structure prediction and FUGUE homology prediction were used to estimate the percentage of helical content that would be expected for each of the HR1 domain constructs. The predicted secondary structure for the HR1 domains determined using the two methods is presented in Table 2 as a comparison for the experimentally determined values.

**Table 2. CD Analysis of the HR1 Domains from the PRK Isoforms**

	helical content <sup>a</sup> (% of residues)			melting temperature (°C)
	experimental	JPred	FUGUE	
PRK1 HR1a	77 <sup>b</sup>	48	54 <sup>c</sup>	46.6 ± 0.3
PRK1 HR1b	55 <sup>b</sup>	59	60 <sup>c</sup>	53.8 ± 0.1
PRK1 HR1ab	53 <sup>b</sup>	56	57 <sup>c</sup>	N/D <sup>d</sup>
PRK2 HR1a	32	45	45	60.1 ± 0.3
PRK2 HR1b	58	59	59	39.8 ± 0.1
PRK2 HR1ab	65	53	53	N/D <sup>d</sup>
PRK3 HR1a	65	57	60	33.2 ± 0.3
PRK3 HR1b	79	64	63	42.9 ± 0.1
PRK3 HR1ab	39	63	64	N/D <sup>d</sup>

<sup>a</sup>Helicity percentages are the total of both  $3_{10}$ -helix and  $\alpha$ -helix. C-Terminal His tags and interdomain linkers were assumed to be unstructured. <sup>b</sup>PRK1 CD data from ref 36 included here for comparison. <sup>c</sup>Experimentally determined from the structures of PDB entries 1cxz and 1urf. <sup>d</sup>Not determined.

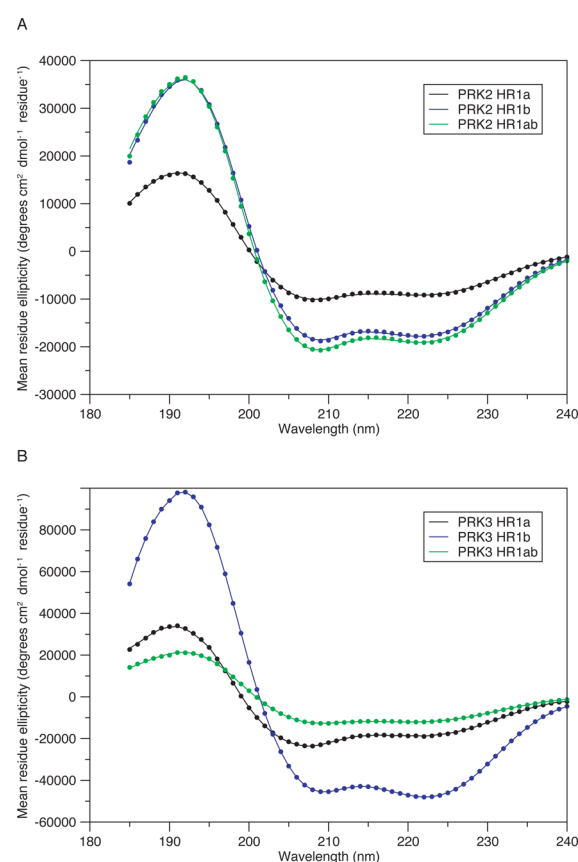


**Figure 5.** CD spectra of the PRK2 and PRK3 HR1 domains: (A) HR1a, HR1b, and HR1ab domains from PRK2 and (B) HR1a, HR1b, and HR1ab domains from PRK3.

CD spectra were collected and analyzed in the same manner for the PRK1 HR1 domains.<sup>36</sup> The CD results (Figure 5), summarized in Table 2, show that the HR1 domains of the PRK isoforms have a variety of helical content, varying from 32 to 79%. The contents of the HR1a domains vary from 32 to 77%, while the contents of the HR1b domains vary from 55 to 79%. The PRK3 HR1a domain and the PRK3 HR1b domain display the highest degree of helicity (65 and 79%, respectively). The PRK2 HR1a domain has the lowest helical content (only 32%). PRK2 and PRK3 HR1 domains have a



secondary structure content different from that of the PRK1 HR1 domains (data included in Table 2 for comparison). The PRK2 HR1a domain has much lower helical content than the PRK1 HR1a domain, while the PRK2 HR1b domain is similar to the PRK1 HR1b domain. The PRK3 HR1 domains appear to have an inverse correlation with the PRK1 domains, with the HR1a domain similar to the HR1b domain and the HR1b domain similar to the HR1a domain. Both the PRK2 HR1b and PRK3 HR1a domains have a secondary structure content similar to that of the PRK1 HR1b domain. The CD analysis of the HR1ab didomain pairs shows that expressing the domains together increases the helical content of PRK2 but decreases the helical content of PRK3, when compared with the helicity of the individual domains. Since there are no published structures for the HR1 domains from PRK2 and PRK3, it is not possible to calculate exactly what percentage of the molecule should be helical, but it is clear from these data that the domains possess a reasonable amount of secondary structure and are likely to be folded coiled-coil domains.

Analysis of the thermal stability of the PRK1 HR1a and HR1b domains gave some insight into why the two domains bind differentially to RhoA and Rac1,<sup>36</sup> so this was repeated for the PRK2 and PRK3 HR1a and HR1b domains. The change in  $\theta_{222}$  with an increase in temperature was monitored, and the data were used to calculate the  $T_m$  values of the PRK2 and PRK3 HR1a and HR1b domains. The results are summarized in Table 2, and the melting curves and their fits are shown in Figure 6. We previously reported a difference of  $\sim 10$  °C

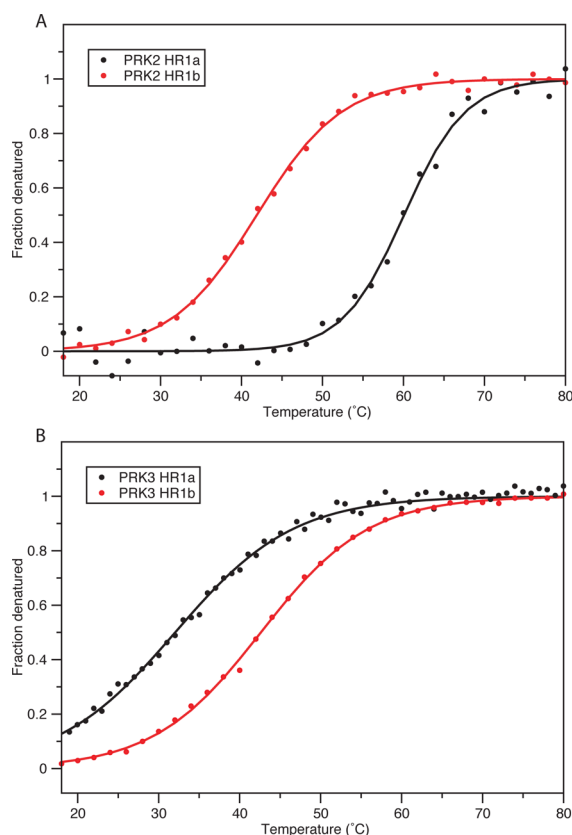


**Figure 6.** Thermal stability of the PRK2 and PRK3 HR1 domains. The melting temperatures were estimated, and the fraction of protein in the denatured state was calculated from the CD signal as described previously:<sup>36</sup> (A) HR1a and HR1b domains from PRK2 and (B) HR1a and HR1b domains from PRK3.

between the  $T_m$  values of the HR1a and HR1b domains of PRK1, with the HR1b domain displaying the higher thermal stability.<sup>36</sup> From the data presented in Table 2, it is clear that the thermal stability of the PRK HR1 domains can be grouped into two classes. PRK2 HR1a falls into the more stable PRK1 HR1b-like category, having a  $T_m$  higher than that of PRK1 HR1b, while PRK2 HR1b, PRK3 HR1a, and PRK3 HR1b have significantly lower thermal stability, closer to that of PRK1 HR1a.

## DISCUSSION

It is known that Rho isoforms RhoA, RhoB, and RhoC interact differentially with effectors *in vivo*.<sup>48</sup> Differences in the effector interactions for the three isoforms have, so far, only tended to have been assessed qualitatively, e.g., using yeast two-hybrid and pull-down assays. The general hypothesis is that differences in subcellular localization are what drive the specificity of the interactions. Little work has been conducted to quantify the differences in the affinities of the Rho isoforms for their effectors. We have previously dissected the interaction between RhoA and PRK1.<sup>36</sup> In this study, we sought to extend that work, looking at the interactions PRK1 makes with RhoB and RhoC, and also to examine the interaction of all three Rho isoforms with the other two members of the PRK family, PRK2 and PRK3.

All three Rho isoforms bind with high (nanomolar) affinity to PRK1 HR1 domains. RhoA and RhoC share the most sequence identity (92%), and indeed, these two proteins have similar affinities for PRK1 HR1 domains. However, RhoB binds both to the HR1a domain alone and to the PRK1 HR1ab didomain significantly more tightly than does RhoA or RhoC (Table 1). The contact residues in the RhoA–PRK1 HR1a interface<sup>36</sup> are completely conserved among the three Rho isoforms (Figure 1B), so it is likely that local differences in the topography of the switch regions allow RhoB to bind more tightly to PRK1. Our data, therefore, indicate that PRK1 is a likely effector protein for all three Rho isoforms but binds with significantly higher affinity to RhoB. The data presented here also confirm that the C-termini of the Rho proteins are not involved in the interaction with PRK1.

On the basis of the analysis of the amino acid sequence of the three PRK isoforms shown in Figure 1C, we predicted that the HR1 domains from PRK2 and PRK3 would bind to Rho family small G proteins in a manner similar to that observed for PRK1. However, the affinities of the PRK2 and PRK3 HR1 domains for all three Rho isoforms were significantly lower than for the PRK1 HR1 domains in almost all cases. The RhoC proteins showed the greatest difference in binding to the three PRK isoforms. Both full-length and truncated RhoC bound tightly to the PRK1 HR1 domains but did not bind with high affinity to the PRK2 HR1 domains or the PRK3 HR1a domain. RhoC bound more tightly to the PRK3 HR1ab didomain, but the interaction is still 5–10-fold weaker than that with PRK1.

The only two residues in the HR1a domain that are involved in contacting RhoA and are significantly different among PRK1, PRK2, and PRK3 are Leu66 in PRK1, which is a Lys in PRK2 and an Arg in PRK3, and Pro72 in PRK1, which is a Tyr in PRK2 and a His in PRK3 (Figure 1C). Both of these residues in PRK1 are at the periphery of the interface with RhoA, so it is unlikely that these substitutions underpin the differences in affinity. However, they do define the end of helix 1 and the start of helix 2 in the PRK1 HR1a domain, so their nonconservation

may reflect slight differences in the helices of the HR1a domains of the PRK isoforms.

All but two of the residues that make energetically important contacts in the RhoA–PRK1 interaction<sup>36</sup> are identical across the PRK isoforms, and those that are not represent conservative changes from leucine to isoleucine. One of the leucine to isoleucine substitutions in PRK2 and PRK3 is the equivalent of Leu52<sup>PRK1</sup>. This residue contacts Tyr66<sup>RhoA</sup> in the RhoA–PRK1 structure, but it is unlikely that such a conservative change would make a difference in the affinity of the PRK2 and PRK3 HR1a domains for RhoA. The other substitution is found in only PRK2 and is the residue equivalent to Leu76<sup>PRK1</sup>. This residue in PRK1 contacts Leu69<sup>RhoA</sup>, but because the affinities of the PRK2 and PRK3 HR1a domains for RhoA are similar, again it is unlikely that substitution of this residue in PRK2 contributes to its reduced affinity for RhoA.

We concluded, therefore, that other features of the interaction interface must result in the PRK2 and PRK3 HR1a domains binding to the Rho family G proteins with an affinity lower than that of the PRK1 HR1 domains. We have observed previously in small G protein–effector interactions that the topography of the binding surface of the small G protein is crucial to formation of a high-affinity complex;<sup>52</sup> presumably, the same can be true of the effector. In fact, we previously concluded with the RhoA–PRK1 complex that flexibility in the HR1a domain appeared to be important for the high-affinity interaction.<sup>36</sup> It is also possible, although unlikely, that the three proteins do not use a conserved interface for binding to the three G proteins.

The PRK2 and PRK3 HR1 constructs designed for this study were all helical as assessed by CD. These domains are expected to form antiparallel coiled coils in a manner similar to that of the HR1 domains from PRK1, and the high degree of secondary structure supports this hypothesis. The decrease in affinity for Rho isoforms, therefore, is not likely to be due to the domains being poorly formed.

The PRK2 HR1a domain was only 32% helical in solution, demonstrating significantly lower secondary structure content than the PRK1 HR1a domain, which was 77% helical in solution. There are nine extra residues at the start of the PRK2 HR1a construct, compared to the PRK1 HR1a construct (Figure 1C). The PRK1 HR1a domain has a short N-terminal helix between residues 14 and 21 that packs against the coiled-coil domain,<sup>32</sup> although this helix is not predicted by JPred and does not appear in FUGUE alignments. If the extra residues in the PRK2 protein have no helical content, this accounts for the lower percentage helicity observed by CD and predicted by JPred and FUGUE.

The PRK3 HR1a domain shows a lower secondary structure content than the PRK1 HR1a domain but significantly higher content than the PRK2 HR1a domain. Its secondary structure content is more similar to that of the PRK1 HR1b domain. The PRK3 HR1a domain does not contain an N-terminal extension; it is in fact 19 residues shorter than the PRK1 HR1a domain and 29 residues shorter than the PRK2 HR1a domain (Figure 1C). Loss of this extension accounts for most of the difference in predicted and experimental helicity.

The results from the analysis of the thermal stabilities of the HR1 domains from PRK2 and PRK3 also gave some surprising results. The data collected for the PRK2 HR1a domain support our previous suggestion that the lower thermal stability of the PRK1 HR1a domain when compared to that of the PRK1 HR1b domain is important for the binding of the PRK1 HR1a

domain to RhoA.<sup>36</sup> The  $T_m$  for PRK2 HR1a was 60 °C and was more similar to the  $T_m$  of the HR1b domain from PRK1 (54 °C) than the  $T_m$  of the PRK1 HR1a domain (47 °C). It may be that the PRK2 HR1a domain binds to RhoA with a lower affinity than the PRK1 HR1a domain because of this increased stability. It could, however, also be that the PRK2 HR1a domain forms a coiled coil where key residues are at positions different from those of the PRK1 HR1a domain, because the measured secondary structure content of the PRK2 HR1a domain was significantly lower than the secondary structure content of the PRK1 HR1a domain. This might alter the accessibility of key residues for G protein binding and hence lower the affinity of PRK2 HR1a for RhoA.

The PRK3 HR1a domain was the least thermally stable of all of the HR1 domains from the three PRK isoforms, with a  $T_m$  of 33.2 °C. On the basis of the hypothesis that a lower thermal stability enhances the binding of HR1 domains to Rho family G proteins, it might be expected that the PRK3 HR1a domain would bind more tightly to Rho proteins than either the PRK1 HR1a domain or the PRK2 HR1a domain. This, however, was not the case. The PRK3 HR1a domain bound to the Rho isoforms with an affinity equivalent to that of the PRK2 HR1a domain. We interpret this to indicate that potentially there is a limit to where increased flexibility will aid binding, at which point the percentage of unfolded molecules in a population will act to decrease affinity. Although some studies have sought to investigate such a correlation, limited data do not at present allow such a link to be established.<sup>53</sup> Structural and functional analysis of the PRK3 protein and how it interacts with Rho proteins will be important in shedding light on its function, especially given its unusual expression patterns.

The HR1b domains from PRK2 and PRK3 were also analyzed for their secondary structure content and thermal stability. The thermal stabilities of both HR1b domains were lower than that of the PRK1 HR1b domain, with values more similar to the  $T_m$  of the PRK1 HR1a domain than to the  $T_m$  of the PRK1 HR1b domain. It is clear that inclusion of the HR1b domains from PRK2 and PRK3 does not affect the affinities of the RhoA and RhoC proteins; however, they do seem to play a role in RhoB binding. It may be that, because the thermal stability of the PRK3 HR1b domain is similar to that of the PRK1 HR1a domain, it allows the PRK3 HR1b domain to participate in the interaction with RhoB. The PRK3 HR1b domain also had a secondary structure content more similar to that of the PRK1 HR1a domain than that of the PRK1 HR1b domain. These data indicate that the PRK3 HR1b domain has biophysical characteristics more suitable for binding to Rho GTPases than the HR1b domains from PRK1 and PRK2.

Possibly, the most interesting result that came out of the study of the interaction between the Rho proteins and the PRK isoforms concerned RhoB. RhoB binds with the highest affinity of all the Rho isoforms to all three PRK isoforms. Although the interaction of RhoB with PRK1 is stronger than that of RhoA or RhoC, the C-terminus of RhoB is not involved. However, the affinity of either truncated or full-length RhoB is higher for HR1ab than for HR1a, implicating the HR1b domain in the PRK1–RhoB interaction. The same pattern is observed with RhoB binding to the PRK2 and PRK3 HR1 domains, although the interactions are clearly more subtle, as truncated RhoB did not show this differential with the domains from PRK3 and with full-length RhoB there was only a small differential with PRK2 domains. Significantly, the PRK3 HR1ab didomain bound 6-fold more tightly to the full-length RhoB protein than

to truncated RhoB. This suggests not only that the PRK3 HR1b domain has a role in binding to RhoB but also that the C-terminus of RhoB may be important for mediating the PRK3 interaction. This is intriguing as the only other description of the involvement of the C-terminal tail of a small G protein in an effector interaction is the complex that forms between Rac1 and PRK1 HR1b.<sup>37</sup> Although the C-terminus of Rho proteins is the region of the protein that is lipid-modified *in vivo*, allowing interaction with the appropriate membrane, it is sterically possible for the residues proximal to the lipid modification sites to be involved in protein–protein interactions.<sup>37</sup> Again overall our data suggest that, on the basis of affinity, PRK2 and PRK3 are likely targets for RhoB rather than RhoA or RhoC. We would also predict that the complexes RhoB forms with both PRK2 and PRK3 would be significantly different from those that form between the Rho isoforms and the PRK1 HR1 domains. Interestingly, a recent study demonstrated that PRK3 may be selective for RhoC, showing an increased level of formation of the complex with RhoC as compared to RhoA and RhoB. Although this study was qualitative, taken together with our results, it may imply that other regions of the PRK isoforms may be important in mediating selective interactions.<sup>26</sup>

All of the data from the binding of the HR1 domains from the PRK isoforms to Rho family G proteins, along with the biophysical data obtained by CD, point to these HR1 domains being more than simple binding modules that bind indiscriminately to Rho proteins; rather, they require other features to drive the specificity of different G protein interactions. Specificity appears to be driven both by local binding surface topography and by domain flexibility rather than solely by surface residue properties, which in many of these protein isoforms are conserved. This was seen initially when comparing the binding of the PRK1 HR1a and HR1b domains to RhoA and Rac1.<sup>32,33,36,37</sup> The PRK1 HR1b domain required the C-terminus of Rac1 to be present to form a high-affinity interaction and was also unable to interact with RhoA, whereas the PRK1 HR1a domain could bind to both G proteins. These differences in binding specificity would not necessarily be unexpected given that the two domains are independent of one another and would, most likely, have evolved to perform different functions.

The differences in binding affinity and thermal stability of the HR1 domains from the PRK isoforms found in this study were more unexpected. When this work was initiated, we hypothesized that because the HR1 domains form simple coiled coils and there was high level of sequence conservation across the helices of the HR1 domains, they would bind in a similar manner to Rho family proteins and with a similar affinity. This is clearly not the case, and the biophysical data from the CD analysis show that, despite their sequence conservation, structurally the HR1 domains from the three isoforms are not equivalent.

Our data also highlight interesting differences in the interactions the PRK isoforms make with RhoB. RhoB has the strongest affinity of all the Rho isoforms for all the PRK isoforms. We observe a likely contribution of the HR1b domain of all PRK isoforms to the interaction with RhoB, which is the first indication that an HR1b domain can influence the interaction with a Rho protein. Our data also suggest that the polybasic tail of RhoB may also participate in the interactions with PRK3, a role for the polybasic region (alternatively known as the hypervariable region) that has only been noted previously in one other small G protein–effector complex.<sup>37</sup>

## AUTHOR INFORMATION

### Corresponding Author

\*Telephone: +44-1223-764824. Fax: +44-1223-766002. E-mail: do@bioc.cam.ac.uk.

### Present Address

||C.L.H.: Philochem AG, Libernstrasse 3, CH-8112 Otelfingen, Switzerland.

### Funding

This research was supported by a BBSRC Studentship to C.L.H. and CR-UK Project Grant C11309/A5148 (to D.O. and H.R.M.).

### Notes

The authors declare no competing financial interest.

## ACKNOWLEDGMENTS

We thank Dr. Joseph Maman (Department of Biochemistry, University of Cambridge) for help with the acquisition of CD data.

## ABBREVIATIONS

RBD, Rho protein binding domain; PRK, protein kinase C-related kinase; HR1, homology region 1; IPTG, isopropyl  $\beta$ -D-thiogalactopyranoside; GST, glutathione S-transferase; GTP, guanosine 5'-triphosphate; GDP, guanosine 5'-diphosphate; DTT, dithiothreitol; SPA, scintillation proximity assay; CD, circular dichroism; PDB, Protein Data Bank.

## REFERENCES

- (1) Ridley, A. J., Allen, W. E., Peppelenbosch, M., and Jones, G. E. (1999) Rho family proteins and cell migration. *Biochem. Soc. Symp.* 65, 111–123.
- (2) Govek, E. E., Newey, S. E., and Van Aelst, L. (2005) The role of the Rho GTPases in neuronal development. *Genes Dev.* 19, 1–49.
- (3) Salminen, A., Suuronen, T., and Kaarniranta, K. (2008) ROCK, PAK, and Toll of synapses in Alzheimer's disease. *Biochem. Biophys. Res. Commun.* 371, 587–590.
- (4) Mueller, B. K., Mack, H., and Teusch, N. (2005) Rho kinase, a promising drug target for neurological disorders. *Nat. Rev. Drug Discovery* 4, 387–398.
- (5) Budzyn, K., Marley, P. D., and Sobey, C. G. (2006) Targeting Rho and Rho-kinase in the treatment of cardiovascular disease. *Trends Pharmacol. Sci.* 27, 97–104.
- (6) Vega, F. M., and Ridley, A. J. (2008) Rho GTPases in cancer cell biology. *FEBS Lett.* 582, 2093–2101.
- (7) Mukai, H., Toshimori, M., Shibata, H., Kitagawa, M., Shimakawa, M., Miyahara, M., Sunakawa, H., and Ono, Y. (1996) PKN associates and phosphorylates the head-rod domain of neurofilament protein. *J. Biol. Chem.* 271, 9816–9822.
- (8) Matsuzawa, K., Kosako, H., Inagaki, N., Shibata, H., Mukai, H., Ono, Y., Amano, M., Kaibuchi, K., Matsuura, Y., Azuma, I., and Inagaki, M. (1997) Domain-specific phosphorylation of vimentin and glial fibrillary acidic protein by PKN. *Biochem. Biophys. Res. Commun.* 234, 621–625.
- (9) Mukai, H., Toshimori, M., Shibata, H., Takanaga, H., Kitagawa, M., Miyahara, M., Shimakawa, M., and Ono, Y. (1997) Interaction of PKN with  $\alpha$ -actinin. *J. Biol. Chem.* 272, 4740–4746.
- (10) Kawamata, T., Taniguchi, T., Mukai, H., Kitagawa, M., Hashimoto, T., Maeda, K., Ono, Y., and Tanaka, C. (1998) A protein kinase, PKN, accumulates in Alzheimer neurofibrillary tangles and associated endoplasmic reticulum-derived vesicles and phosphorylates tau protein. *J. Neurosci.* 18, 7402–7410.
- (11) Metzger, E., Muller, J. M., Ferrari, S., Buettner, R., and Schule, R. (2003) A novel inducible transactivation domain in the androgen receptor: Implications for PRK in prostate cancer. *EMBO J.* 22, 270–280.



- (12) Metzger, E., Yin, N., Wissmann, M., Kunowska, N., Fischer, K., Friedrichs, N., Patnaik, D., Higgins, J. M. G., Potier, N., Scheidtmann, K. H., Buettner, R., and Schule, R. (2008) Phosphorylation of histone H3 at threonine 11 establishes a novel chromatin mark for transcriptional regulation. *Nat. Cell Biol.* 10, 53–60.
- (13) Gao, Q. S., Kumar, A., Srinivasan, S., Singh, L., Mukai, H., Ono, Y., Wazer, D. E., and Band, V. (2000) PKN binds and phosphorylates human papillomavirus E6 oncoprotein. *J. Biol. Chem.* 275, 14824–14830.
- (14) Bourguignon, L. Y. W., Gilad, E., Peyrollier, K., Brightman, A., and Swanson, R. A. (2007) Hyaluronan-CD44 interaction stimulates Rac1 signaling and PKN $\gamma$  kinase activation leading to cytoskeleton function and cell migration in astrocytes. *J. Neurochem.* 101, 1002–1017.
- (15) Lachmann, S., Jevons, A., De Rycker, M., Casamassima, A., Radtke, S., Collazos, A., and Parker, P. J. (2011) Regulatory Domain Selectivity in the Cell-Type Specific PKN-Dependence of Cell Migration. *PLoS One* 6, e21732.
- (16) Schmidt, A., Durgan, J., Magalhaes, A., and Hall, A. (2007) Rho GTPases regulate PRK2/PKN2 to control entry into mitosis and exit from cytokinesis. *EMBO J.* 26, 1624–1636.
- (17) Calautti, E., Grossi, M., Mammucari, C., Aoyama, Y., Pirro, M., Ono, Y., Li, J., and Dotto, G. P. (2002) Fyn tyrosine kinase is a downstream mediator of Rho/PRK2 function in keratinocyte cell-cell adhesion. *J. Cell Biol.* 156, 137–148.
- (18) Wallace, S. W., Magalhaes, A., and Hall, A. (2011) The Rho Target PRK2 Regulates Apical Junction Formation in Human Bronchial Epithelial Cells. *Mol. Cell Biol.* 31, 81–91.
- (19) Palmer, R. H., and Parker, P. J. (1995) Expression, Purification and Characterization of the Ubiquitous Protein-Kinase-C-Related Kinase-1. *Biochem. J.* 309, 315–320.
- (20) Quilliam, L. A., Lambert, Q. T., MickelsonYoung, L. A., Westwick, J. K., Sparks, A. B., Kay, B. K., Jenkins, N. A., Gilbert, D. J., Copeland, N. G., and Der, C. J. (1996) Isolation of a NCK-associated kinase, PRK2, an SH3-binding protein and potential effector of Rho protein signaling. *J. Biol. Chem.* 271, 28772–28776.
- (21) Palmer, R. H., Ridden, J., and Parker, P. J. (1995) Cloning and Expression Patterns of 2 Members of a Novel Protein-Kinase-C-Related Kinase Family. *Eur. J. Biochem.* 227, 344–351.
- (22) Oishi, K., Mukai, H., Shibata, H., Takahashi, M., and Ono, Y. (1999) Identification and characterization of PKN $\beta$ , a novel isoform of protein kinase PKN: Expression and arachidonic acid dependency are different from those of PKN $\alpha$ . *Biochem. Biophys. Res. Commun.* 261, 808–814.
- (23) Leenders, F., Mopert, K., Schmiedeknecht, A., Santel, A., Czauderna, F., Aleku, M., Penschuck, S., Dames, S., Sternberger, M., Rohl, T., Wellmann, A., Arnold, W., Giese, K., Kaufmann, J., and Klippel, A. (2004) PKN3 is required for malignant prostate cell growth downstream of activated PI 3-kinase. *EMBO J.* 23, 3303–3313.
- (24) Aleku, M., Schulz, P., Keil, O., Santel, A., Schaeper, U., Dieckhoff, B., Janke, O., Endruschat, J., Durieux, B., Roder, N., Löffler, K., Lange, C., Fechtner, M., Mopert, K., Fisch, G., Dames, S., Arnold, W., Jochims, K., Giese, K., Wiedenmann, B., Scholz, A., and Kaufmann, J. (2008) Atu027, a Liposomal Small Interfering RNA Formulation Targeting Protein Kinase N3, Inhibits Cancer Progression. *Cancer Res.* 68, 9788–9798.
- (25) Mopert, K., Löffler, K., Roder, N., Kaufmann, J., and Santel, A. (2012) Depletion of protein kinase N3 (PKN3) impairs actin and adherens junctions dynamics and attenuates endothelial cell activation. *Eur. J. Cell Biol.* 91, 694–705.
- (26) Unsal-Kacmaz, K., Ragunathan, S., Rosfjord, E., Dann, S., Upeklis, E., Grillo, M., Hernandez, R., Mack, F., and Klippel, A. (2012) The interaction of PKN3 with RhoC promotes malignant growth. *Mol. Oncol.* 6, 284–298.
- (27) Collazos, A., Michael, N., Whelan, R. D. H., Kelly, G., Mellor, H., Pang, L. C. H., Totty, N., and Parker, P. J. (2011) Site recognition and substrate screens for PKN family proteins. *Biochem. J.* 438, 535–543.
- (28) Gavard, J., and Gutkind, J. S. (2008) Protein Kinase C-related Kinase and ROCK Are Required for Thrombin-induced Endothelial Cell Permeability Downstream from Ga(12/13) and Ga(11/q). *J. Biol. Chem.* 283, 29888–29896.
- (29) Fujisawa, K., Madaule, P., Ishizaki, T., Watanabe, G., Bito, H., Saito, Y., Hall, A., and Narumiya, S. (1998) Different regions of Rho determine Rho-selective binding of different classes of Rho target molecules. *J. Biol. Chem.* 273, 18943–18949.
- (30) Watanabe, G., Saito, Y., Madaule, P., Ishizaki, T., Fujisawa, K., Morii, N., Mukai, H., Ono, Y., Kakizuka, A., and Narumiya, S. (1996) Protein kinase N (PKN) and PKN-related protein rhotilin as targets of small GTPase Rho. *Science* 271, 645–648.
- (31) Mukai, H. (2003) The structure and function of PKN, a protein kinase having a catalytic domain homologous to that of PKC. *J. Biochem.* 133, 17–27.
- (32) Maesaki, R., Ihara, K., Shimizu, T., Kuroda, S., Kaibuchi, K., and Hakoshima, T. (1999) The structural basis of Rho effector recognition revealed by the crystal structure of human RhoA complexed with the effector domain of PKN/PRK1. *Mol. Cell* 4, 793–803.
- (33) Owen, D., Lowe, P. N., Nietlispach, D., Brosnan, C. E., Chirgadze, D. Y., Parker, P. J., Blundell, T. L., and Mott, H. R. (2003) Molecular dissection of the interaction between the small G proteins Rac1 and RhoA and protein kinase C-related kinase 1 (PRK1). *J. Biol. Chem.* 278, 50578–50587.
- (34) Flynn, P., Mellor, H., Palmer, R., Panayotou, G., and Parker, P. J. (1998) Multiple interactions of PRK1 with RhoA: Functional assignment of the HR1 repeat motif. *J. Biol. Chem.* 273, 2698–2705.
- (35) Blumenstein, L., and Ahmadian, M. R. (2004) Models of the cooperative mechanism for Rho effector recognition: Implications for RhoA-mediated effector activation. *J. Biol. Chem.* 279, 53419–53426.
- (36) Hutchinson, C. L., Lowe, P. N., McLaughlin, S. H., Mott, H. R., and Owen, D. (2011) Mutational Analysis Reveals a Single Binding Interface between RhoA and Its Effector, PRK1. *Biochemistry* 50, 2860–2869.
- (37) Modha, R., Campbell, L. J., Nietlispach, D., Buhecha, H. R., Owen, D., and Mott, H. R. (2008) The Rac1 polybasic region is required for interaction with its effector PRK1. *J. Biol. Chem.* 283, 1492–1500.
- (38) Vincent, S., and Settleman, J. (1997) The PRK2 kinase is a potential effector target of both Rho and Rac GTPases and regulates actin cytoskeletal organization. *Mol. Cell Biol.* 17, 2247–2256.
- (39) Lu, Y., and Settleman, J. (1999) The Drosophila Pkn protein kinase is a Rho Rac effector target required for dorsal closure during embryogenesis. *Genes Dev.* 13, 1168–1180.
- (40) Shibata, H., Oishi, K., Yamagiwa, A., Matsumoto, M., Mukai, H., and Ono, Y. (2001) PKN $\beta$  interacts with the SH3 domains of Graf and a novel Graf related protein, Graf2, which are GTPase activating proteins for Rho family. *J. Biochem.* 130, 23–31.
- (41) Mach, H., Middaugh, C. R., and Lewis, R. V. (1992) Statistical Determination of the Average Values of the Extinction Coefficients of Tryptophan and Tyrosine in Native Proteins. *Anal. Biochem.* 200, 74–80.
- (42) Fenwick, R. B., Prasannan, S., Campbell, L. J., Nietlispach, D., Evetts, K. A., Camonis, J., Mott, H. R., and Owen, D. (2009) Solution Structure and Dynamics of the Small GTPase RalB in Its Active Conformation: Significance for Effector Protein Binding. *Biochemistry* 48, 2192–2206.
- (43) Graham, D. L., Eccleston, J. F., and Lowe, P. N. (1999) The conserved arginine in Rho-GTPase-activating protein is essential for efficient catalysis but not for complex formation with rho CDP and aluminum fluoride. *Biochemistry* 38, 985–991.
- (44) Whitmore, L., and Wallace, B. A. (2004) DICHROWEB, an online server for protein secondary structure analyses from circular dichroism spectroscopic data. *Nucleic Acids Res.* 32, W668–W673.
- (45) Whitmore, L., and Wallace, B. A. (2008) Protein secondary structure analyses from circular dichroism spectroscopy: Methods and reference databases. *Biopolymers* 89, 392–400.



- (46) Compton, L. A., and Johnson, W. C. (1986) Analysis of Protein-CD Spectra for Secondary Structure Using a Simple Matrix Multiplication. *Biophys. J.* 49, A494.
- (47) Sreerama, N., and Woody, R. W. (2000) Analysis of protein CD spectra: Comparison of CONTIN, SELCON3, and CDSSTR methods in CDPPro software. *Biophys. J.* 78, 334A.
- (48) Wheeler, A. P., and Ridley, A. J. (2004) Why three Rho proteins? RhoA, RhoB, RhoC, and cell motility. *Exp. Cell Res.* 301, 43–49.
- (49) Shi, J. Y., Blundell, T. L., and Mizuguchi, K. (2001) FUGUE: Sequence-structure homology recognition using environment-specific substitution tables and structure-dependent gap penalties. *J. Mol. Biol.* 310, 243.
- (50) Jeanmougin, F., Thompson, J. D., Gouy, M., Higgins, D. G., and Gibson, T. J. (1998) Multiple sequence alignment with Clustal x. *Trends Biochem. Sci.* 23, 403–405.
- (51) Larkin, M. A., Blackshields, G., Brown, N. P., Chenna, R., McGettigan, P. A., McWilliam, H., Valentin, F., Wallace, I. M., Wilm, A., Lopez, R., Thompson, J. D., Gibson, T. J., and Higgins, D. G. (2007) Clustal W and clustal X version 2.0. *Bioinformatics* 23, 2947–2948.
- (52) Elliot-Smith, A. E., Mott, H. R., Lowe, P. N., Laue, E. D., and Owen, D. (2005) Specificity Determinants on Cdc42 for Binding Its Effector Protein ACK. *Biochemistry* 44, 12373–12383.
- (53) Teilum, K., Olsen, J. G., and Kragelund, B. B. (2011) Protein stability, flexibility and function. *Biochim. Biophys. Acta* 1814, 969–976.
- (54) Barton, G. J. (1993) Alscript: A Tool to Format Multiple Sequence Alignments. *Protein Eng.* 6, 37–40.